Design of a Shim for a Nanopositioner

by

Corey G. Harris

Submitted to the Department of Mechanical Engineering in Partial Fulfillment of the
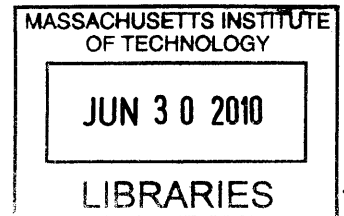Requirements for the Degree of

Bachelor of Science

at the

Massachusetts Institute of Technology

June 2010

©2010 Corey G. Harris
All rights reserved
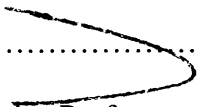
Signature of Author...................................
Department of Mechanical Engineering
May 19, 2010

Certified by...................................
Martin Culpepper
Associate Professor of Mechanical Engineering
Thesis Supervisor

Accepted by...........
John H. Lienhard V
ins Professor of Mechanical Engineering
Chairman, Undergraduate Thesis Committee

Design of a Shim for a Nanopositioner

by

Corey G. Harris

Submitted to the Department of Mechanical Engineering
on May 19, 2010 in Partial Fulfillment of the
Requirements for the Degree of Bachelor of Science in
Mechanical Engineering

ABSTRACT

The purpose of this thesis is to assist in the development of a low cost nanopositioner by designing a specific component – a shim that is located in the scan tip assembly of the nanopositioner. Nanopositioners must maximize precision to successfully produce features of fewer than 100 nm. The kinematic coupling used to place the tool tip is capable of producing a high level of precision across tool changes, assuming the groove mount is held in place. It is therefore very important to secure the groove mount to prevent dislocation and enhance the viability of nano-scale device fabrication. The shim developed within this thesis serves to secure the groove mount of the kinematic coupling, which was previously held in place solely with magnetic attraction. The shim secures the groove mount by applying a force to the side of the groove mount in addition to increasing the magnetic attraction between the groove mount and universal mount of the nanopositioner. It was first modeled with solid and magnetic modeling software before being manufactured and tested. With the addition of the shim, the vertical force required to displace the groove mount increased by a factor of 9.4, from 0.14 N to 1.29 N. Similarly the lateral force increased by a factor of 27.9, from 0.09 N to 2.45 N. As a result, the nanopositioner is significantly better suited to perform its function. The nanopositioner will be used to produce nano-scale devices including carbon nanotubes, molecular actuators, and transistors, with applications across several disciplines. Future work includes developing a tool to bend the shim tabs and simplify the manufacturing process.

Thesis Supervisor: Martin Culpepper

Title: Associate Professor of Mechanical Engineering

Acknowledgements

I would like to take a moment to thank those that made this possible. Without the help of these people, my success would not have been assured.

To my advisor, Professor Martin Culpepper, thank you for allowing me to take on this project. I appreciate your advice and guidance and I learned a lot from you.

To the Shop Guys, Pat and Dave, thanks for all your support over the years. Your willingness to help people is an asset to the Institute.

To Mrs. Sandra Tenorio, thank you for accepting my MITES application. The program prepared me for what was to come and opened my eyes to exploring new opportunities.

Special thanks to my parents, Curtis and Alcha Harris, for their continued love and support in all my endeavors. I live to make you proud.

Table of Contents

List of Figures

Chapter 1: Introduction

1.1 Purpose

The purpose of this thesis is to design and optimize a shim that is capable of securing the groove mount of a kinematic coupling used in a nanopositioner. The nanopositioner uses a kinematic coupling to maintain a high level of precision as the tool is removed and replaced. The shim design is particularly interesting because it employs both mechanical and magnetic properties to secure the groove mount. By holding the groove mount in place, the shim makes it possible for the nanopositioner to maintain its precision throughout the fabrication of various nano-scale devices. These devices, including carbon nanotubes, molecular actuators, and transistors, have an ever increasing array of applications ranging from medicine to the semiconductor industry.
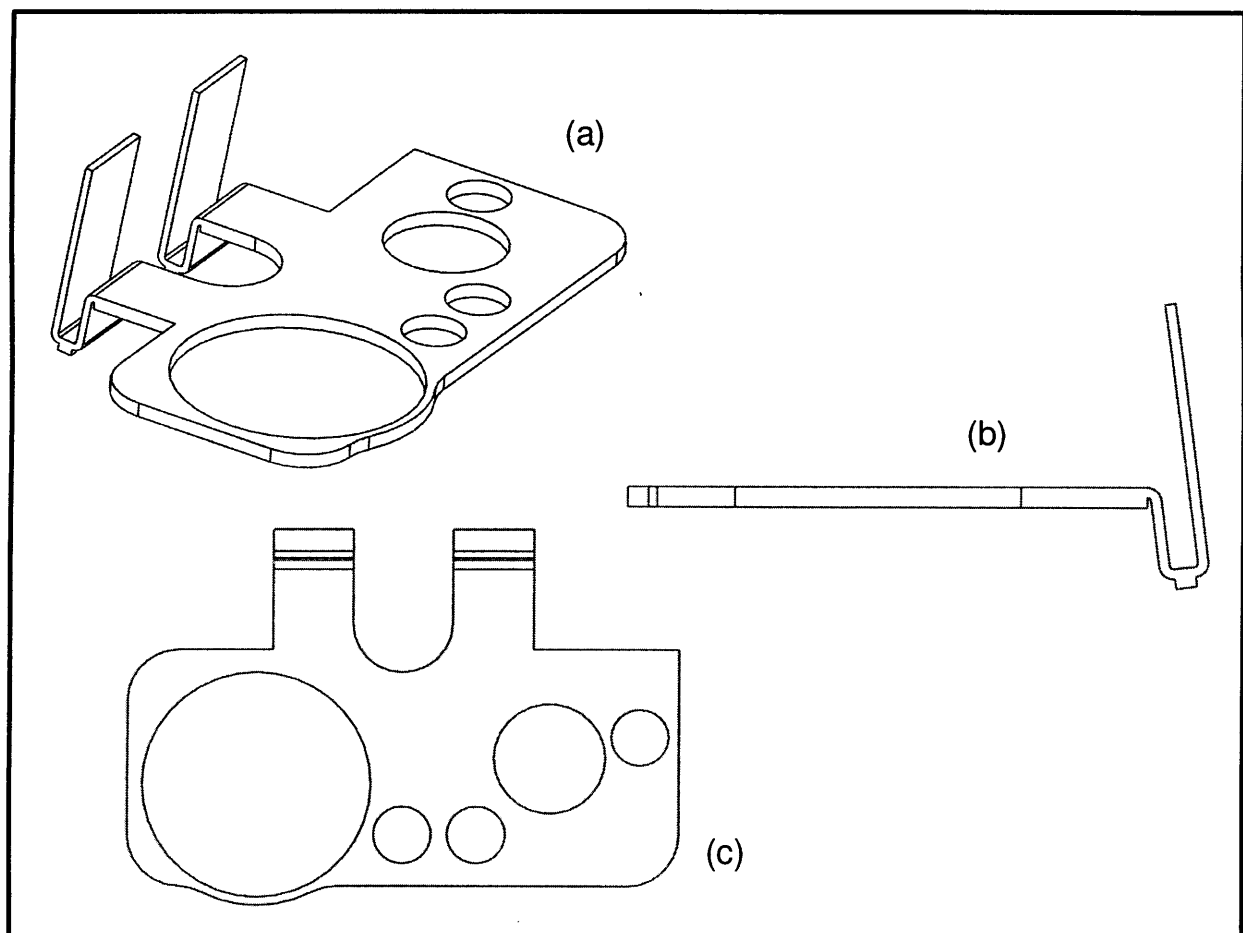
Figure 1: Shim Design: (a) Isometric, (b) Top View, and (c) Side View.
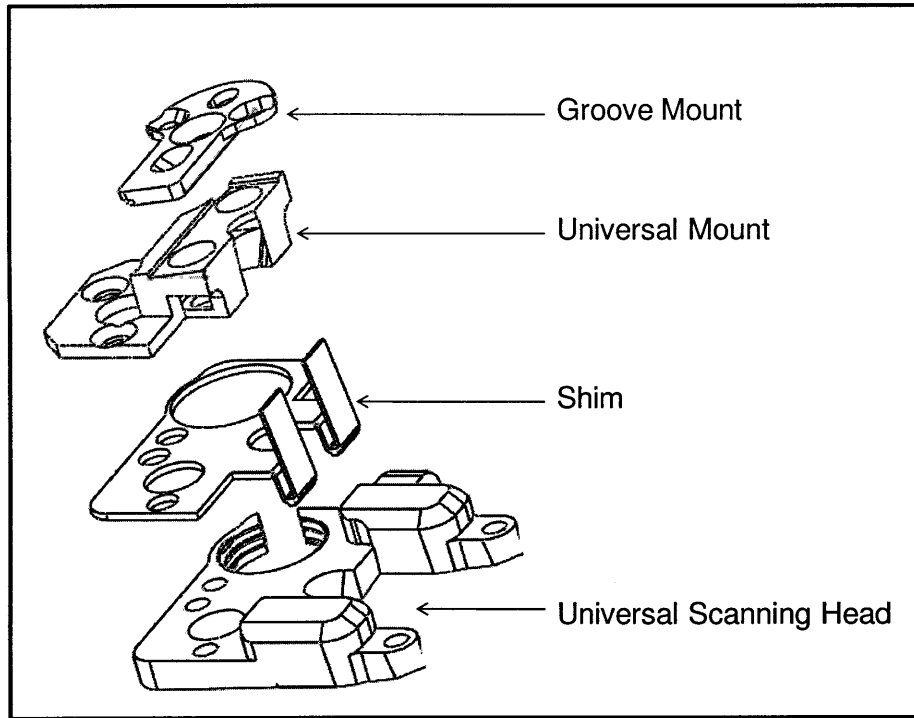
Figure 2: Exploded view of Scan Tip Assembly with Shim.

The shim is sandwiched between the universal scanning head and the universal mount (see Fig 2). The shim tabs interface with the groove mount and secure it by (1) by applying a mechanical preload to the side of the groove mount and (2) by augmenting the magnetic attraction between the groove mount and the universal mount. The shim was optimized such that it would successfully perform its function (quantified in section 1.6) without decreasing the performance of the nanopositioner. Its properties are summarized in Table 1, below.

Table 1: Summary of Shim properties.

Property	Value
Mass (g)	0.3
Max Deflection (mm)	0.26
Max Load (N)	0.83
Design Deflection (mm)	0.2
Mechanical Load (N)	1.27
Dislocation Force (N)	
·Vertical	1.29
·Lateral	2.45

1.2 Background

Manufacturing processes help turn designs into actual products. They range from simple to complex but all fundamentally change the form of starting materials into another form so that they may achieve a particular function. The industrial age in particular brought a need for improvements in manufacturing. With increases in technology there was the need and the ability to produce things faster and with better quality. This development led to many of the familiar processes we have today - machining, die casting, and welding to name a few. The industrial age was over a hundred years ago. Old processes have been improved or made obsolete and new process have been introduced.

Dip-Pen Nanolithography is a new manufacturing process that makes possible the deposition of molecules onto a substrate on scales of fewer than one hundred nanometers. It works by using a meniscus to place molecules onto a substrate in a manner similar to the way a quill pen writes ink on paper. Many manufacturing processes rely on breaking things down, also called "top-down" processes. Two examples are cutting a piece of wood and drilling a hole for a screw. With this new process, it is possible to build things from the "bottom up", on a near atomic level. Dip-Pen Nanolithography has applications in several areas including medicine, electronics, and the semiconductor industry. As the understanding of nanotechnology increases, the potential applications of this new technology are increasing as well.

A nanopositioner is the mechanical device required to achieve the level of precision necessary to perform Dip-Pen Nanolithography. A novel nanopositioner has been designed that uses a reluctance based actuator and a Hexflex positioning stage to achieve the desired level of precision. The tool tip of the nanopositioner is mounted on a kinematic coupling which is held to a universal mount by magnetic forces. In early iterations, there were issues with the groove mount becoming displaced across tool changes. The shim developed within this thesis is meant to solve this problem by physically securing the groove mount in addition to enhancing the magnetic force holding the groove mount in place.

1.3 Development of Idea

The nanopositioner design employs a kinematic coupling to position the tool tip. The kinematic coupling in this nanopositioner is made up of a ball mount, coupling balls, and a groove mount.

11

The coupling balls rest in three grooves on the groove mount and the ball mount rests on top of the coupling balls. In the finished coupling, the balls are glued to the ball mount. If the ball mount is taken off the groove mount and then reseated, the position will be within nanometers of the original position. This high level of precision is one of the benefits of using a kinematic coupling. Used in this configuration, it ensures that the ball mount ends up in virtually the same position relative to the groove mount, regardless of human error in placing the ball mount.

Though the kinematic coupling was successful in increasing the precision across tool changes, it relied on the groove mount staying in place. Before the introduction of the shim, the groove mount was only held in place solely by magnets embedded in the universal mount. During operation and across tool changes, it was easy to dislocate the groove mount and even remove it completely. Magnetic attraction only resists lateral forces through friction and thus has poor control in securing the groove mount in the presence of external lateral forces. The ball mount contained a magnet that attracted it to the universal mount when it was in place. This magnet also attracted the groove mount. In this manner, while the magnet was necessary during operation, its effects were a nuisance during tool changes when the entire kinematic coupling would be removed instead of just the ball mount.

The first idea was to selectively increase the magnetic attraction between the groove mount and the universal mount. The increased magnetic attraction would hold the groove mount in place more firmly and outweigh the effects of the ball mount magnet during tool changes. The increased magnetic attraction would also mitigate some of the lateral dislocation. There was no room to install additional magnets so the problem was approached from a different angle. Instead of increasing the strength of the magnetic field, the magnetic field and corresponding flux would be channeled through the groove mount and back to the magnets within the universal mount, thereby increasing the magnetic force holding the groove mount in place. This would be accomplished by decreasing the reluctance along a path from the magnet to the groove mount. A metallic shim was proposed as a solution with tabs that would direct the magnetic flux to pass through the groove mount and back to the magnets within the universal mount.

Preliminary estimates showed that the magnetic force could be increased by a factor of 5.6. The additional attraction would be significant. Before this idea was optimized, however, the lateral

12

dislocation of the groove mount resurfaced as an issue. The first idea was one good solution, but was there a better one? Could a shim prevent the lateral dislocation too?

The next idea was an attempt to solve two problems with one component. The idea was that the tabs used to redirect magnetic flux could also be used to mechanically secure the groove mount. By designing the tabs such that they pressed against the side of the groove mount, the lateral dislocation issue could be eliminated. In addition, the shim would be even better at directing flux through the groove mount because the two components would be in contact. The shim was developed from this idea and is the subject of this thesis.

1.4 Shim Description

The shim is a thin piece of 17-7 PH stainless steel machined and formed to optimize its performance. The shim is sandwiched between the universal scanning head and the universal mount (see Fig. 1 & 2). Tabs coming from the base are bent up to interface with the groove mount. When the groove mount is put in place, it displaces the shim tabs resulting in an applied force against the groove mount. The groove mount was previously held in place only by weak magnetic forces from two Alnico magnets embedded in the universal mount. With the addition of the shim, the vertical force required to displace the groove mount increased by a factor of 9.4, from 0.14 N to 1.29 N. Similarly the lateral force increased by a factor of 27.9, from 0.09 N to 2.45 N.

1.5 Thesis Organization

The paper proceeds with the functional requirements and how they led to the corresponding design parameters. The following sections detail the tuning of these parameters for mechanical and magnetic optimization of the shim. The thesis then closes with a brief discussion of the results and areas for future work.

Chapter 2: Design

2.1 Design Requirements

The function of the shim is to hold the groove mount in place both during machine operation and when it is necessary to remove the ball mount, only. It achieves this by applying a preload to the side of the groove mount while simultaneously increasing the magnetic attraction between the groove mount and the universal mount. The shim must achieve these functions without negatively affecting the performance of the machine. The main constraints are geometric as the shim must fit within a small space and remain clear of the laser beam of the nanopositioner. It also must successfully deal with the environmental conditions in which it will be present, including chemical and thermal considerations.
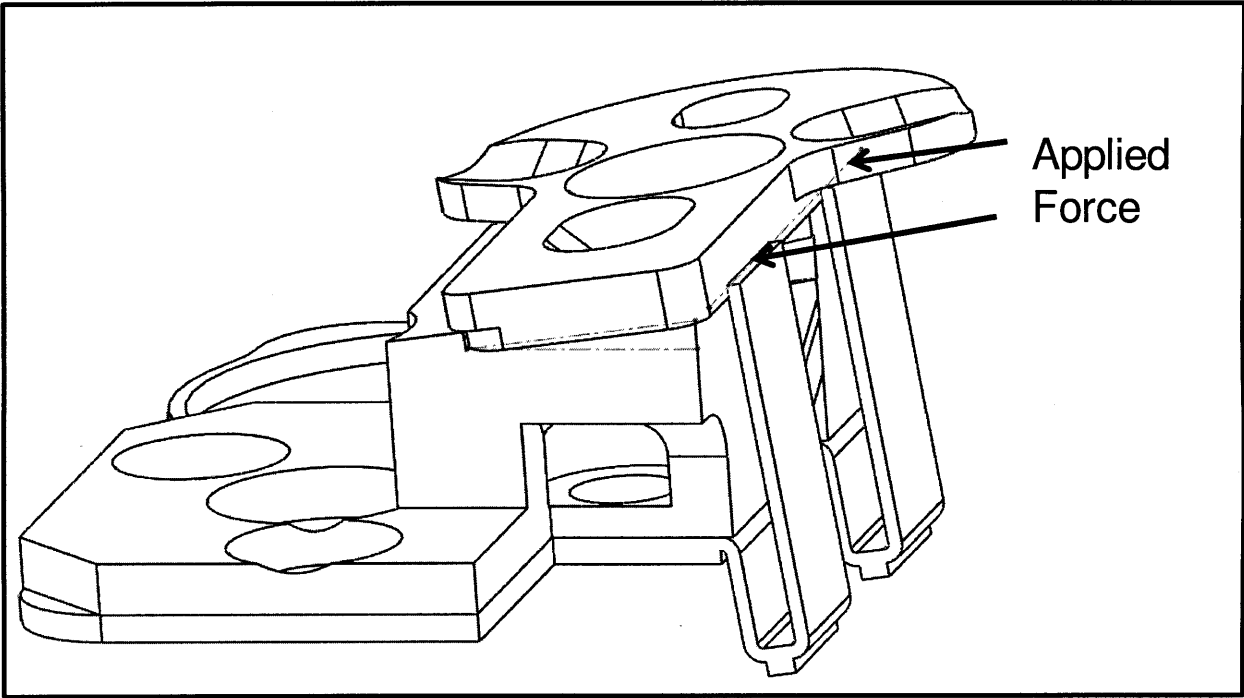
Figure 3: The shim tabs apply a load to the side of the groove mount, securing it in place.
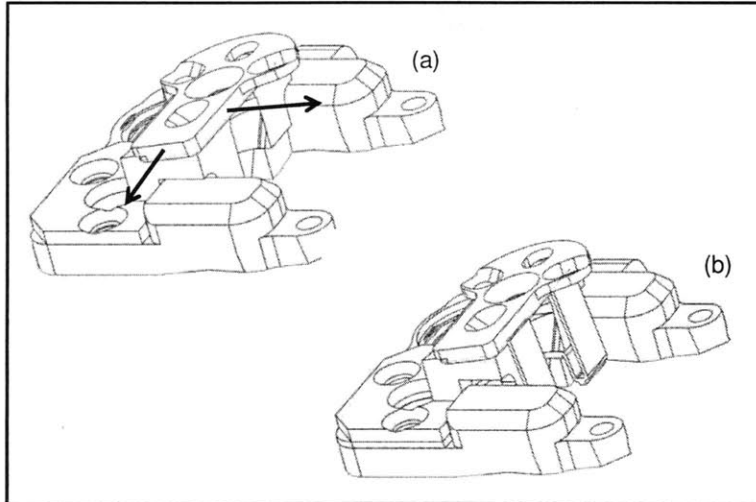
Figure 4: Scan Tip Assembly: (a) Without shim, the groove mount can easily move laterally. (b) With shim, the groove mount is held in place.

Corrosion resistance

Dip-Pen Nanolithography applies chemicals to a substrate to create nanostructures. The materials in close proximity to the scan tip must possess a base level of resistance to the potentially damaging effects of the chemicals involved.

Tab Deflection Range – 0.20-0.30 mm

The tabs on the shim apply a force related to the amount of deflection they experience. In order to maintain performance over the lifetime of the nanopositioner, the deflection should not produce a stress great enough to yield the material. A deflection of 0.20 mm (0.0079 in) is required to hold the groove mount in place. The additional 0.10 mm (0.0039 in) is included to decrease the likelihood of the material undergoing yield during groove mount placement. The closer the range is to 0.20 mm (0.0079 in), the higher the securing force will be.

Tab Force Range – 0.50 N to 1.50 N

Each tab applies a force to the groove mount that serves to hold it in place across tool changes. The mass of the groove mount is 0.24 grams resulting in a gravitational force of 2.4×10^{-3} N. Despite the low magnitude, the suggested range is two orders of magnitude above the required force to hold the weight of the groove mount. For this reason, a combined applied force of 1-3 N from both tabs should be adequate to secure the shim. It should be noted that excessive force is

15

equally undesirable to a weak force because excessive force would hinder the intentional removal of the groove mount.

Mass – < 5 g

The shim must fit within a small operational envelope. Excessive weight should be avoided.

Design Temperature Range – 15-25 C

Due to the nature of nanotechnology, nanolithography typically occurs under well controlled environmental conditions. Though various temperatures may be used in the fabrication process, the temperature is not likely to exceed these bounds while the tool is being changed.

Lifetime

The shim shall be designed to operate successfully over the life of the nanopositioner. Replacement should only be required if the shim is stressed beyond its design envelope.

2.2 Material Selection

In selecting a material for the shim it was necessary to pick a material that would have the best opportunity to meet the design criteria. The material needed to have a high strength to weight ratio in addition to being corrosion resistant. This quickly narrowed the selection to stainless steels. Our particular selection, 17-7 precipitate hardened steel, was chosen for its high strength, corrosion resistance, and formability. The high ultimate tensile strength to yield strength ratio made it possible to bend the tabs without material failure. This type of stainless steel is also ferromagnetic, which is beneficial in strengthening the magnetic attraction between the groove mount and universal mount. The relevant material properties are highlighted in Table 1 below.

Table 2: Material properties for 17-7 PH Stainless Steel

Material Properties	
Density	7.8 g/cc
Tensile Yield Strength	276 Mpa
Ultimate Tensile Strength	896 Mpa
Young's Modulus	204 Gpa
CTE	11 μm/m•°C

16

2.3 Magnetic Design Theory

Magnetism is a complex phenomenon that is difficult to model without the assistance of computer programming. It is possible to approximate magnetic behavior in simple cases, particularly where symmetry is involved, but software must be used to properly model the majority of situations. Despite this reality, the fundamental equations provide a sense of how best to take magnetic considerations into the design approach.

For the purpose of designing the shim, obtaining the exact characteristics of the magnetic flux is unnecessary; the attraction between the groove mount and the universal mount is the main concern. In this regard, observing the equations of magnetic force provides insight into how best to approach optimization. The magnetic force, F_m, between two magnetized objects is given by

$$F_m = \frac{\varphi^2 A}{2\mu_0} .$$

[1]

The magnetic force can thus be increased most readily by increasing the magnetic flux passing through the two objects. Magnetic flux is given by

$$\varphi = \frac{V_m}{R} ,$$

[2]

where R is the magnetic reluctance. Reluctance in magnetic circuits in analogous to resistance in electric circuits – just as current flows through the path of least resistance, flux flows through the path of least reluctance. For a given magnetomotive force, supplied by the magnet, it is possible to increase the magnetic flux by decreasing the reluctance. Reluctance is given by

$$R = \frac{l}{\mu_r \mu_0 A_{cs}},$$

[3]

where μ_r is the magnetic permeability of the material. Ferromagnetic materials have significantly higher permeability than air. These formulas add validity to the idea of using the shim tabs to channel flux such that it passes through the groove mount and increases the magnetic attraction.

17

2.4 Mechanical Design

The shim works by supplying a preload against the side of the groove mount. The geometry of the tabs determines how the applied force relates to the deflection. The arrangement of the shim between the universal mount and the universal scanning head causes limited mobility for the sandwiched region. The tabs can be modeled as a series of cantilevered beams because the base of the shim is immobile. More specifically, the geometry of the tabs may be analyzed with the assistance of Homogenous Transformation Matrices, or HTM's. In this manner, the tip deflection caused by the placement of the groove mount can be linked to the applied force using material mechanics.

2.4.1 Homogeneous Transformation Matrices (HTM's)

The shim tabs were modeled with the aid of Homogeneous Transformation Matrices or HTM's. HTM's can be used to convert the coordinates of a particular point from one reference frame to another. The general 2D translational and rotational matrix is given by Equation [4].

$$\begin{bmatrix} A' \\ B' \\ 1 \end{bmatrix} = \begin{bmatrix} cos\theta & sin\theta & \Delta x \\ -sin\theta & cos\theta & \Delta y \\ 0 & 0 & 1 \end{bmatrix} \cdot \begin{bmatrix} A \\ B \\ 1 \end{bmatrix} \qquad [4]$$
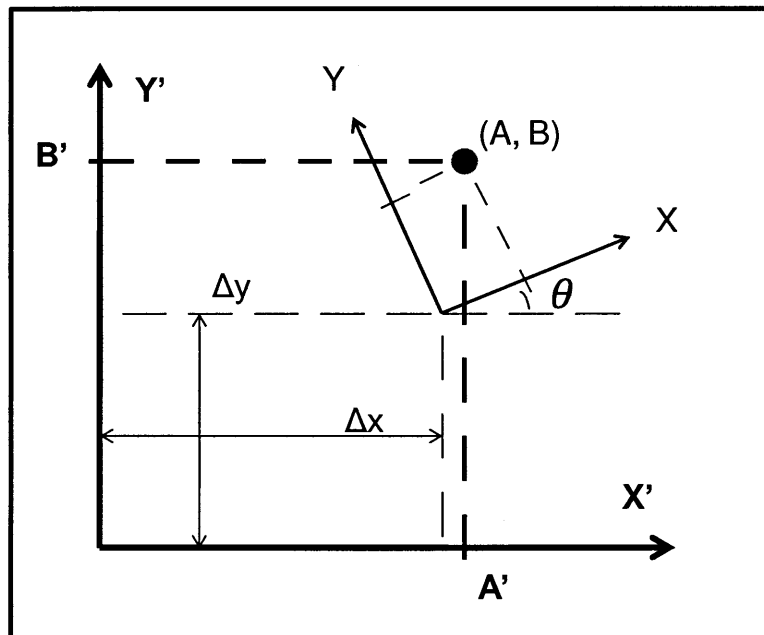
Figure 5: Transformation diagram for 2D HTM.

18

By incorporating the beam bending equations into the matrices, it is possible to identify the position of a point of interest relative to a frame of our choosing. In this case, the point of interest is the tip of the shim tab and the frame is a stationary frame located at the beginning of the tab.
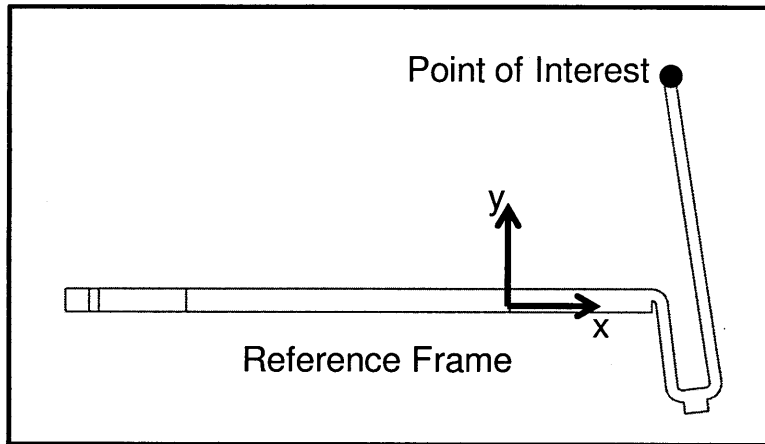
Figure 6: Reference Frame and Point of Interest of the Shim.

The material properties are incorporated by modeling each segment of the tab as a cantilevered beam. A force is applied to the tip of the shim tab and equilibrium analysis is performed to find the forces and moments in each section of the tab. These forces and moments are then converted to displacements and angles using the equations in Figure 7. Once the HTM's are formed, they can be entered into a computer program, such as MathCAD or MatLab, and used to generate deflection data (see Appendix B).

The equations shown are:

$$d = \frac{FL}{EA}$$

$$d = \frac{FL^3}{3EI} \qquad \theta = \frac{FL^2}{2EI}$$

$$d = \frac{ML^2}{2EI} \qquad \theta = \frac{ML}{EI}$$

Figure 7: Deflection equations for forces and moments applied to the end of a beam.

19

2.5 Shim Tab Geometry

The general dimensions of the shim were predetermined by the geometry of the scan tip assembly. The base of the shim must have the same profile as the top of the universal scanning head. In addition, the shim tabs must fit between the actuators within the universal scanning head. The surface of the universal mount, and thus the groove mount, is skewed at 7° from normal. The geometry of the shim tab was selected by tracing the edge of the groove mount until it intersected with the plane of the base of the shim.
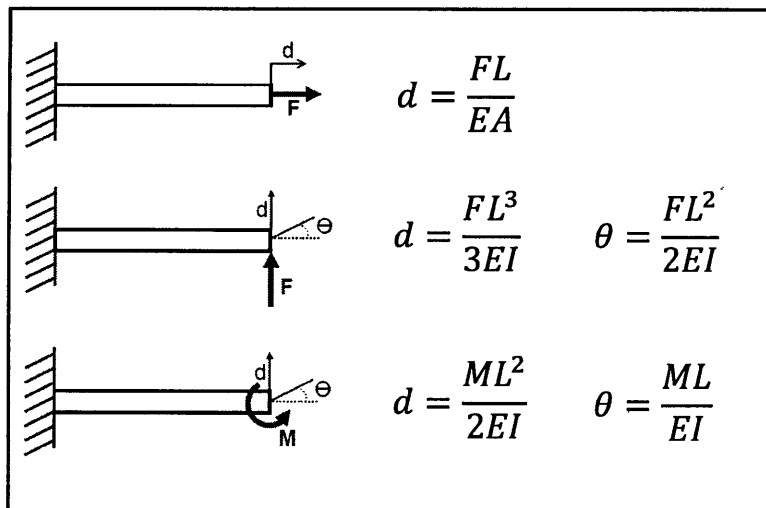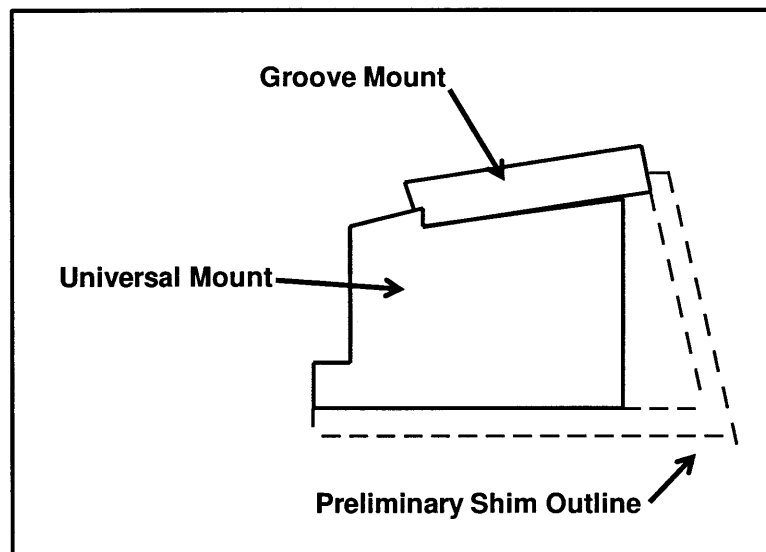

Figure 8: Preliminary Shim form envelope.

Once the solid model was created, the shim tab was angled so that it touched the edge of the universal mount. When the groove mount is placed on the universal mount, the tabs deflect and apply a force. There are many ways to select an initial shape or set of shapes, but this manner has the advantage of being relatively simple and thus efficient to model and optimize.

The shim tab acts like a cantilevered beam with a force applied to the tip at a right angle. By integrating the elastic curve equation and plugging in initial conditions, the lateral force, F, is found to be related to the deflection, δ, by

$$F = \frac{3EI\delta}{L^3} .$$
[5]

20

The maximum stress in a beam is related to the applied moment and the geometry of the beam. It can be found by substituting the corresponding variables into the flexure formula:

$$\sigma_{max} = \frac{FLt}{2I} \quad .$$

[6]

Combining [5] and [6] yields the following:

$$t = \frac{2\sigma_{max}}{3E\delta} L^2 \quad .$$

[7]

Equation [7] was evaluated using the material properties of stainless steel, and it was quickly discovered that the length dimension was too small to undergo the required deflection without yielding the material. Using the distance prescribed by the shim outline as the beam length (Fig. 8), the maximum tab thickness required to prevent yielding is calculated to be about 14 microns! Even if the precision could be achieved, a component with such a small thickness would be easy to break during and after the machining process. The maximum thickness is proportional to the square of the length (Eq. [7]). This relationship means that increasing the length could make fabrication a lot more practical.

The current design makes uses of a nested flex tab mechanism to get the additional required length without having to machine the tab to an impossibly small dimension. The outline of the shim tab was extended and made to curve back to the base of the shim. The effective length of the tab is roughly the sum of the two flex tab lengths because the tabs are roughly parallel to each other.
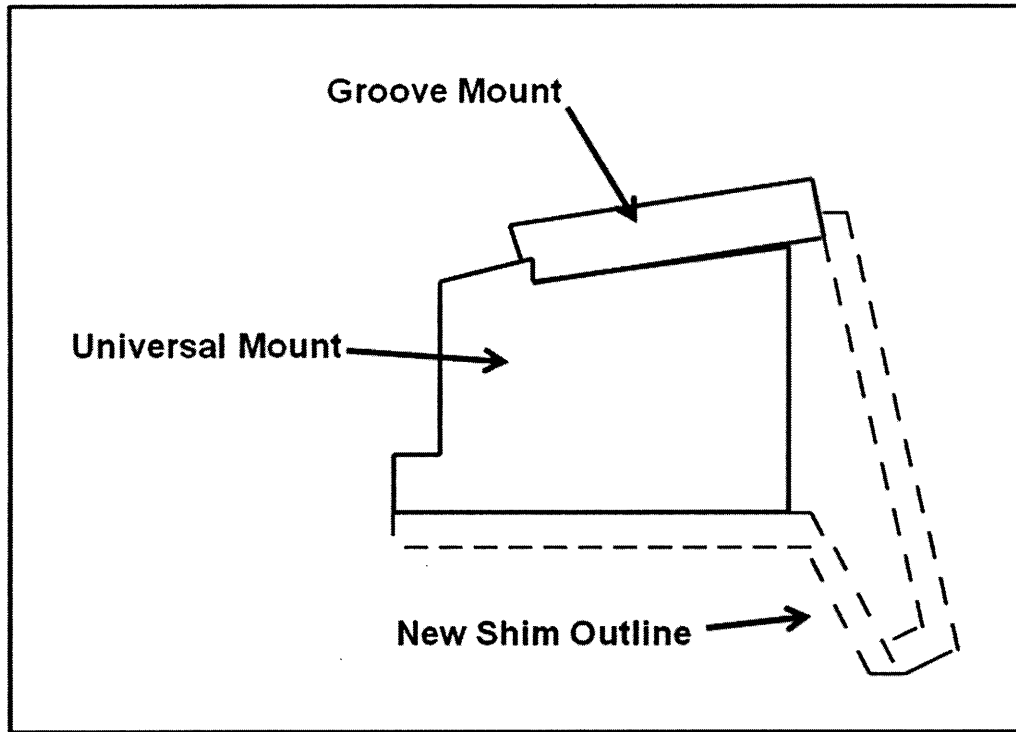
Figure 9: Shim Outline with nested tab that increases the effective length of the shim tab.

Chapter 3: Modeling, Optimization, and Manufacture

3.1 Mechanical Modeling and Optimization

The mechanical modeling and optimization were performed with the assistance of both MathCAD and SolidWorks.

3.1.1 MathCAD

MathCAD is an engineering calculation program with the ability to perform matrix operations. The software is particular useful for its support of both IPS and MKS units. The process began by entering the HTM's and relevant variables into the worksheet. Once the general shape of the shim has been determined, the modeling takes on a methodical form. The shim is divided into four sections (see Fig. 10). The base section matches the dimensions of the base of the universal scanning head and has a thickness of 0.41 mm (0.016 in). The widths of the tabs are maximized to minimize stress. The tab itself is divided into three sections. There are two sections that are meant to flex and one section that is meant to transfer the force between the flex tabs. The optimal thickness of the flex tabs was determined to be 0.20 mm (0.008 in) from magnetic modeling, but experience has shown that this is around the limit capable of withstanding the forces associated with normal handling. The spacer is 0.41 mm (0.016 in) thick to ensure a higher stiffness in relation to the shim tabs. These dimensions, in addition to supporting the function of the shim, have the added benefit of supporting design-for-manufacturing philosophy. The changes in thickness make it easier to bend the tabs at the correct location. Once all these variables were entered into the worksheet, the optimal length of the shim tab was the only thing left to determine.
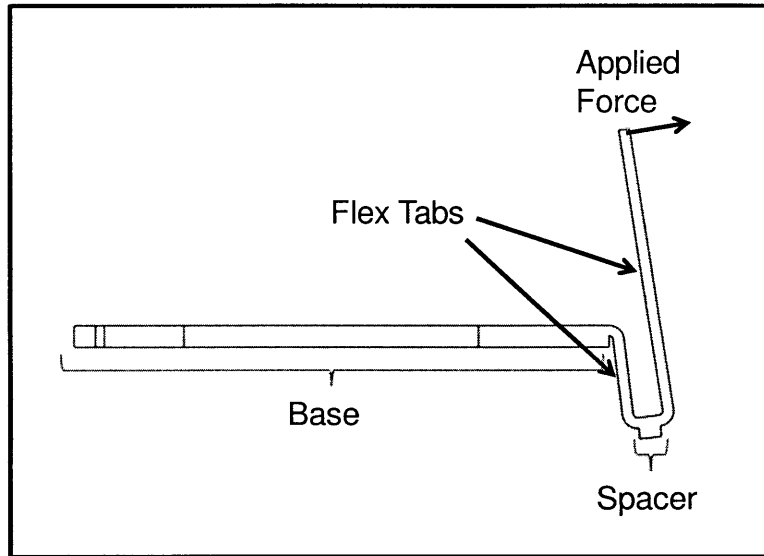
Figure 10: Shim sections. The applied force is meant to be absorbed by the two flex tab sections.
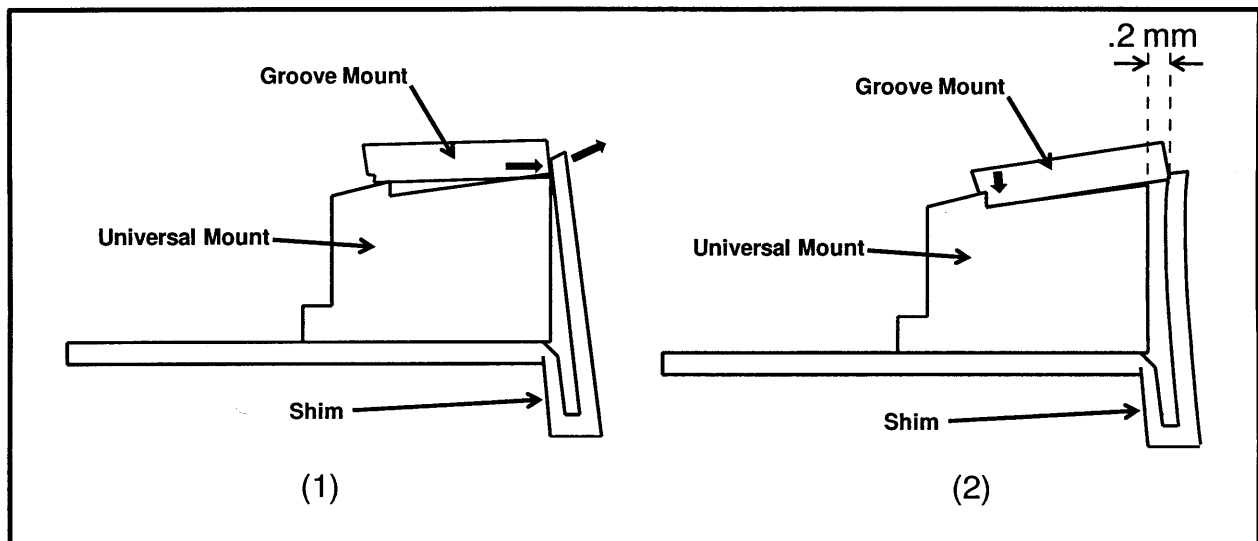
Figure 11: The groove mount is placed by placing a corner into the pocket created by the shim tab and the top of the universal mount. The groove mount locks into place by first sliding sideways against the shim tab (1) and then down (2).

The shim is designed to press against the side of the universal mount when the groove mount is not in place. The action of sliding the groove mount into position bends the tabs by 0.20 mm (0.0079 in) (see Fig. 11). The tab length is determined by the balance of two opposing forces. Decreasing the tab length increases the applied force which makes the groove mount less likely to become displaced. Increasing the length, however, increases the deflection range of the shim tab. In order to have both the applied force and the deflection fall within the desired range, it is

necessary to understand how the tab length affects the stiffnss of the shim tab. By experimenting with different lengths in the MathCAD software, it was discovered that a tab length of 5.61 mm (0.2209 in) corresponded to a force of 0.83 N and a deflection of 0.25 mm (.0098 in). This configuration met the design requirements. It is possible to get slightly more force from the shim tabs, but this increases the risk of yielding the shim tabs.

3.1.2 SolidWorks

SolidWorks is a 3D mechanical CAD program with the ability to simulate deformation under applied loading. The shim was modeled by using the various tools within the software to replicate the shape and form of the design, which was output from MathCAD. The constraints and loading configuration were loaded into the software. Then a mesh was generated and the solver analyzed the design for both deformation and stress.

The simulation was performed using a large displacement analysis and the FFEPlus solver. The SolidWorks model predicted a tip displacement of 0.26 mm (0.0102 in) for an applied loading of 0.83 N. The MathCAD model predicted the shim tip would displace by 0.25 mm (.0098 in) for the same force. SolidWorks is better equipped for solid modeling. Taking the SolidWorks model as the actual measurement produces an error or 4.5% between the two software predictions, which is acceptable.
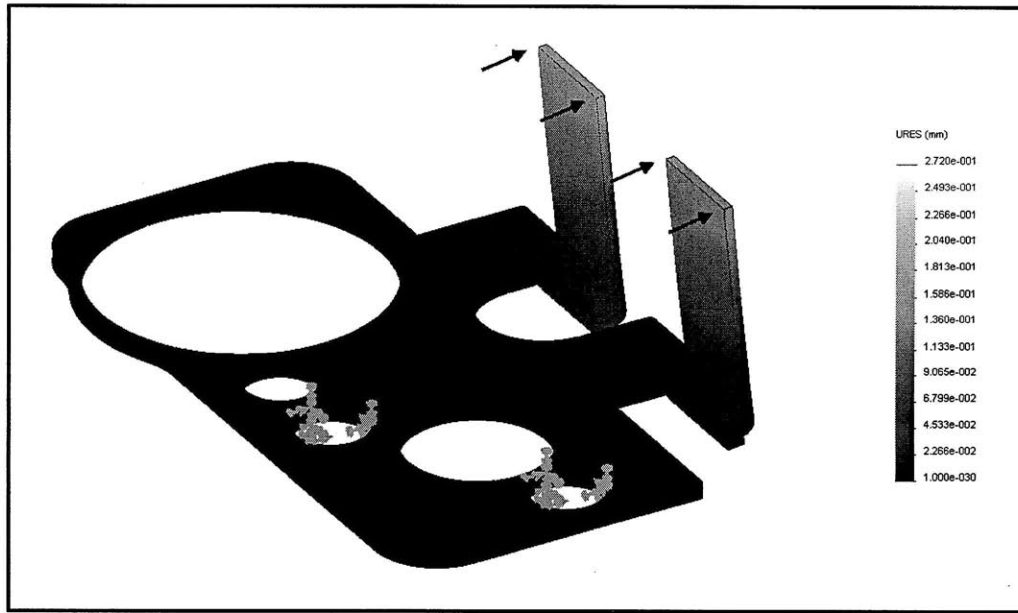
Figure 12: SolidWorks screenshot of shim with load applied. The deflection predicted by MathCAD was 4.5% less than the deflection predicted by SolidWorks.

The models were compared at the point just prior to yield. The force in operation is not the maximum force but the force corresponding to a 0.20 mm (0.0079 in) deflection. The SolidWorks anticipates a force of 0.64 N per tab resulting in a total force of 1.27 N.

3.2 Magnetic Modeling

The material was modeled with Femm version 4.2. Femm is a 2D magnetic modeling program that is capable of extending its calculations to symmetric components. Our model was not symmetric and thus contains an inherent level of inaccuracy. In addition the material was modeled as 416 steel instead of 17-7 PH Stainless. The two materials have similar chemical composition to warrant this comparison.

The magnetic modeling process is similar to other FEA programs. The geometry of the shim was obtained from the corresponding DXF file generated by SolidWorks. The material properties were assigned and boundary conditions set. Then the mesh was created and the analysis performed. The results were consistent with our understanding of magnetic behavior.

Without the shim, flux from the magnet is spread out in space. In this configuration, the flux is left unharnessed as shown in Figure 13.

26
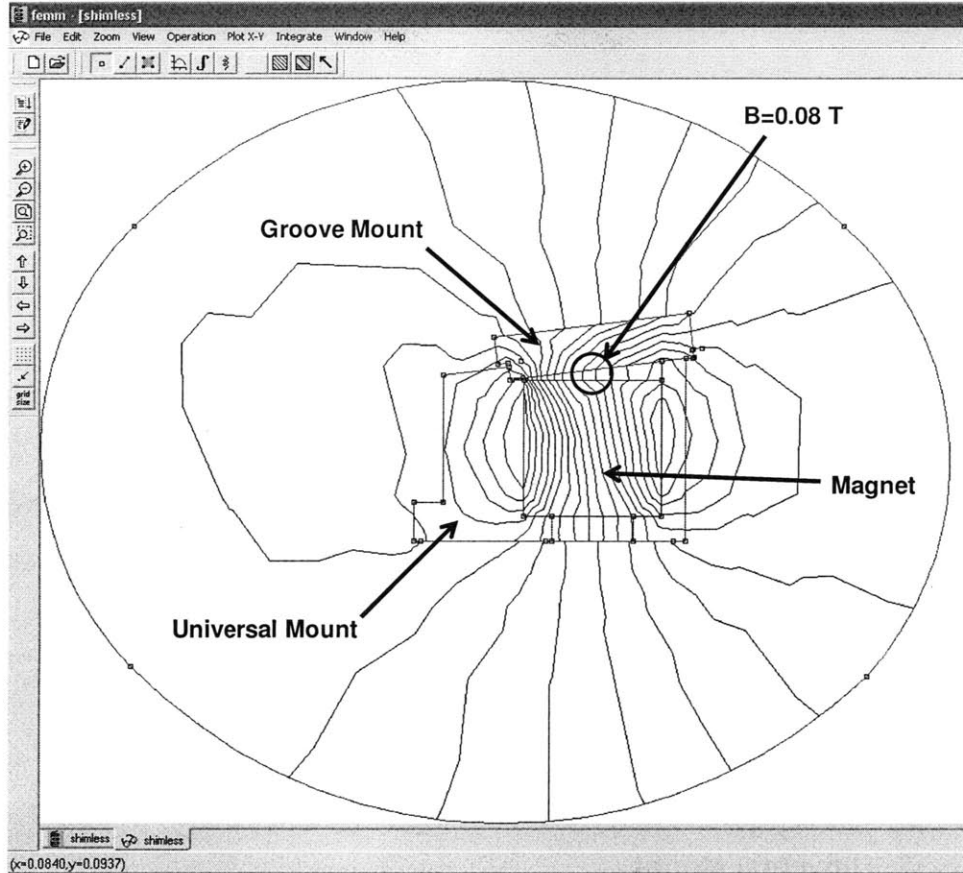
Figure 13: Femm screenshot of shim-less model. The magnetic flux measured at the center of the groove mount is 0.08 T.

In the preliminary design, the shim achieved its function solely through decreasing the magnetic resistance surrounding the groove mount. This resulted in increased flux being channeled through the groove mount holding it in place. In this configuration, there was no contact between the shim tabs and the groove mount despite close proximity, as shown in Figure 14. The air gap between the shim tabs and the groove mount provided resistance to the magnetic flux and resulted in some of the flux becoming dispersed instead of passing through the groove mount. This configuration is better than the shim-less configuration, but remains less than ideal.
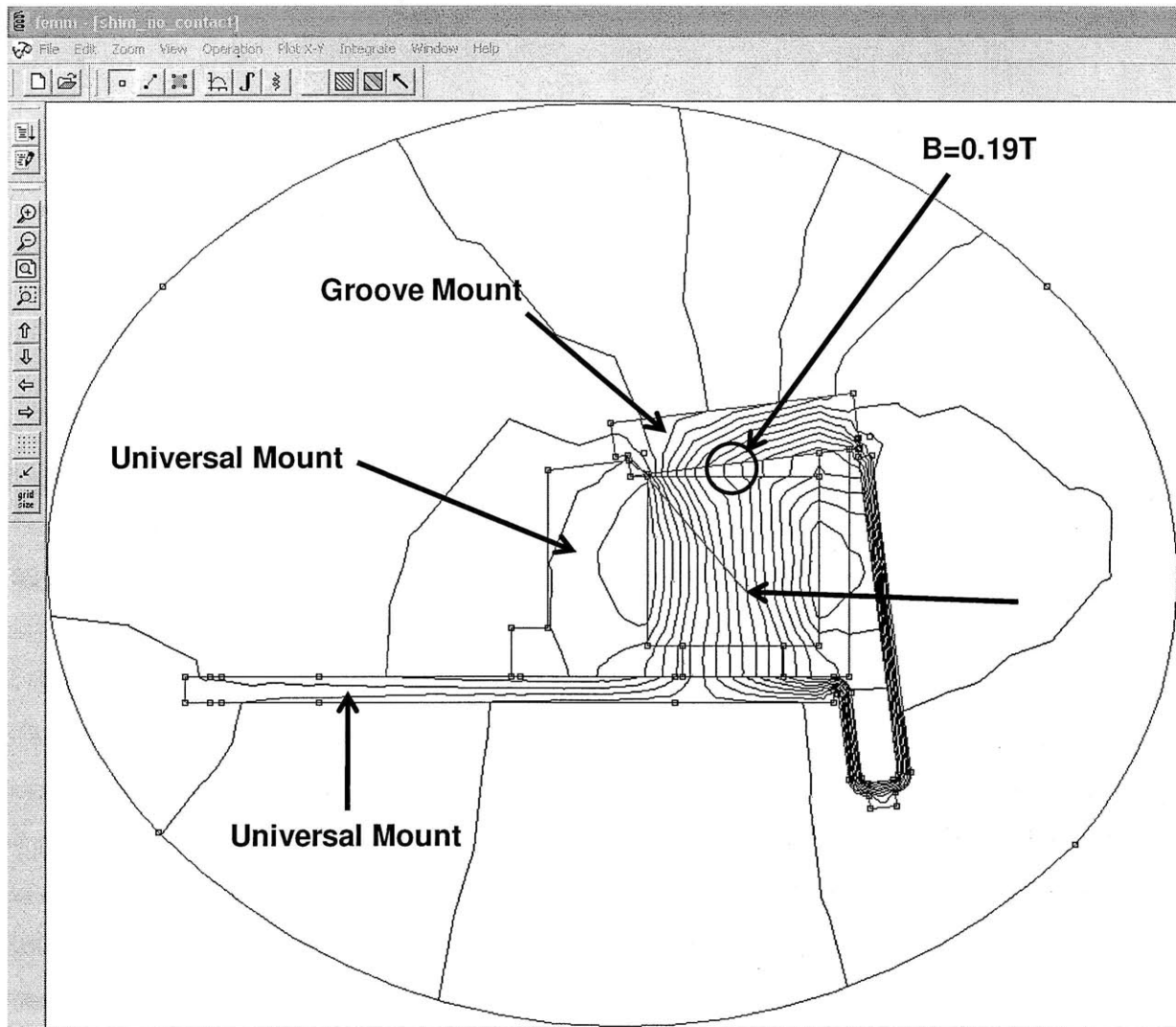
Figure 14: Femm screenshot with shim present, but not contacting the groove mount. The magnetic flux passing through the groove mount increased to 0.19 T.

In the new design, the shim is in contact with the groove mount. The flux has a direct path from the magnet to the groove mount. The majority of the flux is channeled through the shim tabs into the groove mount as shown in Figure 15.
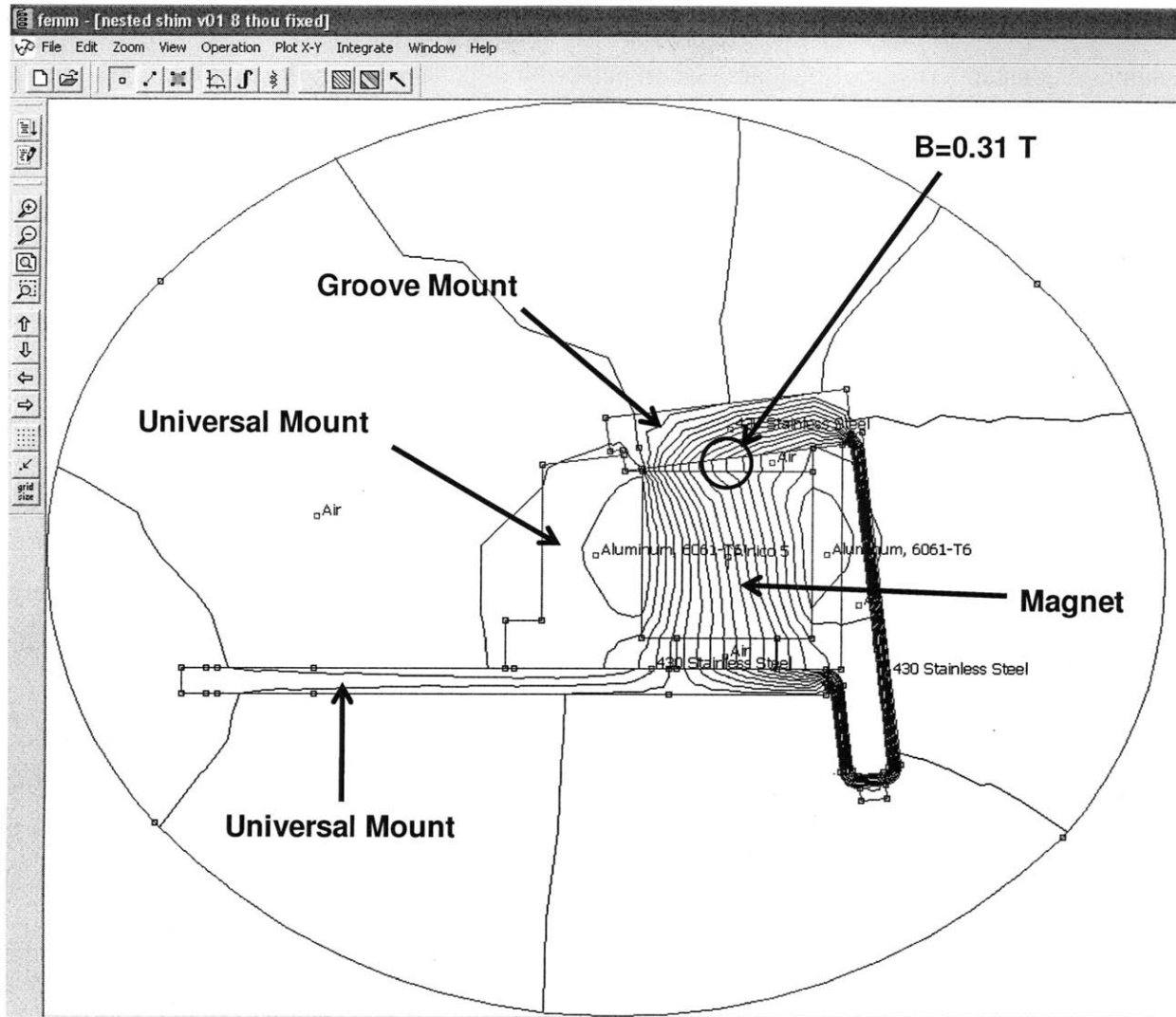
Figure 15: Femm screenshot showing magnetic flux with shim. The magnitude taken at the center of the groove mount is 0.31 T.

The decision to use the shim tabs to mechanically secure the groove mount inherently increased the magnetic force holding the groove mount in place. The parameter of interest became the thickness of the tabs. When a conductive material experiences a magnetic field, domains within the material align and the material becomes magnetized. The level of magnetization is directly related to the strength of the magnetic field. There is a limit, however, beyond which the material cannot be further magnetized. This happens when all the domains have been aligned and so further recruitment is impossible. Increasing the magnetic field further will result in dispersion of the flux as the material cannot contain any more.

The magnetic model was created from a cross section of the scan tip assembly. The software assumes a constant cross sectional area when performing its analyses. It is safe to design to the saturation point because the shim has a rectangular cross section while the magnet is cylindrical – excess flux can still pass through the sides of the shim tabs which are further from the magnet and receive less direct flux. It is also beneficial to have the shim as thin as possible to concentrate the flux through the groove mount. Different thicknesses were modeled and a thickness of 0.20 mm (0.008 in) was determined to be the saturation limit.

3.3 Manufacture

The shim was produced from a piece of 0.41 mm (0.016 in) thick, 17-7 PH stainless steel. The shim was first cut out using CNC Milling machine and a 1.59 mm (0.0625 in) end mill. The operation was run at a fraction of the typical feeds and speeds to prevent the piece from breaking. The shim was designed such that it could be cut out flat and then bent into the desired shape. The small envelope simplified the machining.
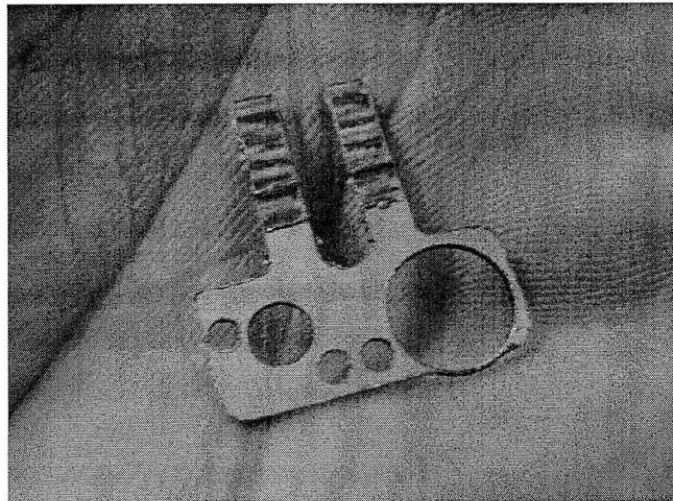
Figure 16: Shim cut from 0.41 mm (0.016 in) thick, 17-7 PH stainless steel sheet. The mill left a small burr which was easily removed with a file.

After it was cut on the mill, it was bent using a pair of pliers to the desired angle as measured by a protractor.
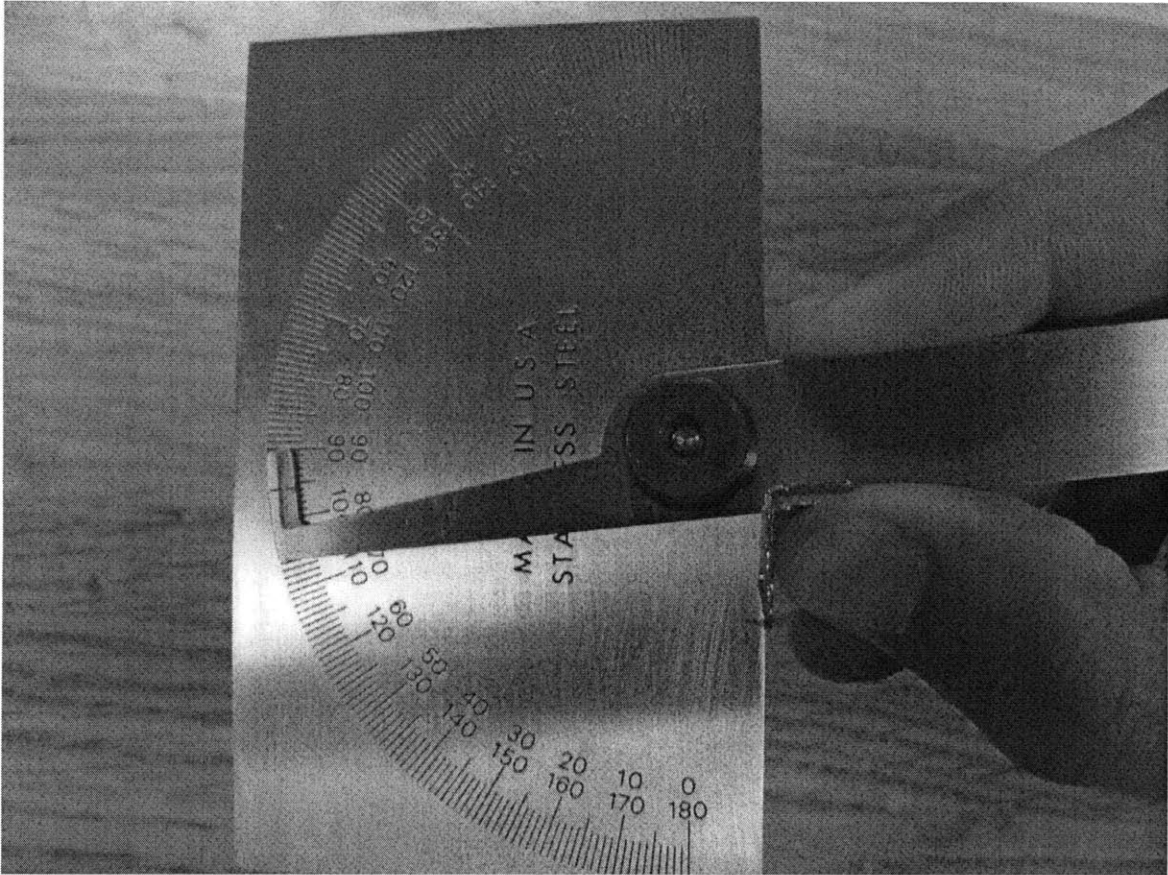
Figure 17: Shim being measured after being bent with pliers. The shim was bent to 7 degrees and then tuned.

The shim is designed in such a manner that plastic deformation is concentrated in the corners of the bends and not dispersed throughout the shim. For this reason, the shim is relatively forgiving if the desired angle is missed. The length of the tabs provides for a wide envelope of error. The stainless steel used for the shim also has an elongation of 35%. This means that the steel exhibits a decent degree of ductility which helps to prevent the tabs from breaking. Once the tabs are bent into shape, the shim is placed between the universal scanning head and the universal mount. The three components are held together with two screws.

Chapter 4: Validation

4.1 Testing

The shim was tested to measure how well the shim solved the initial problem. Testing was performed by looping a thin wire through a hole in the groove mount and hanging masses from it in vertical and lateral orientations. The mass hanging from the wire was increased until the groove mount slipped. The process was repeated after the groove mount had been reseated using gradually decreasing mass increments to zero in on the maximum mass.
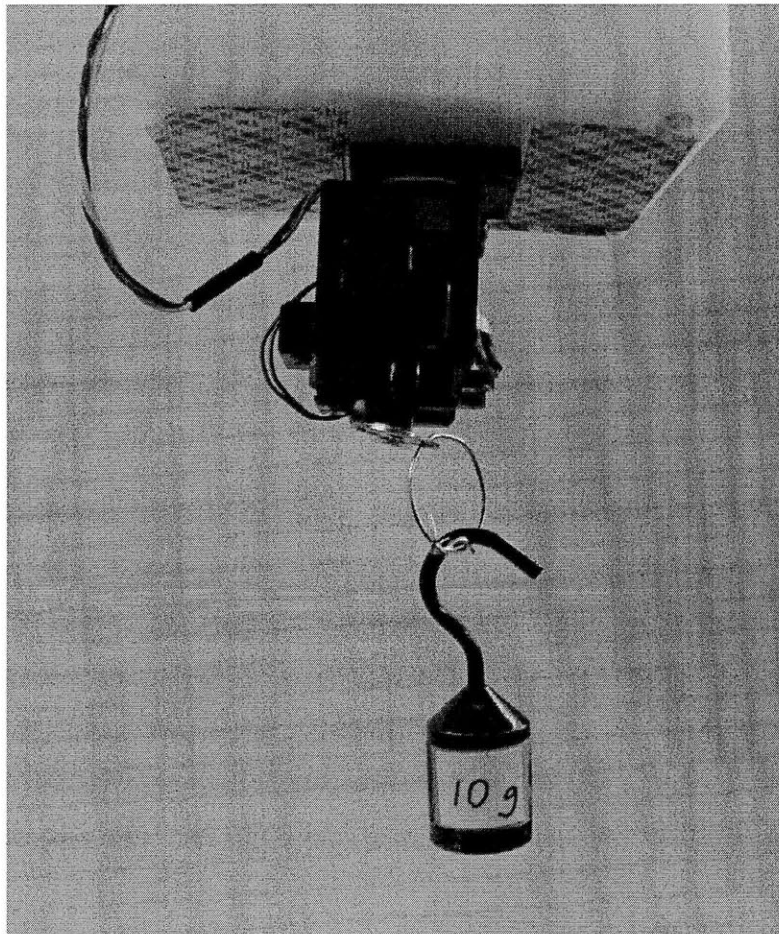
Figure 18: Vertical loading condition with 10 g mass.

Paperclips were used to get the maximum mass value within one gram. After the same maximum mass was recorded three times, the mass was weighed with a balance. These maximum values were converted to forces using the acceleration of gravity and recorded in Table 2.

Orientation	Force (N)		Ratio
	Shim	No Shim	
Vertical	1.29	0.14	9.4
Lateral	2.45	0.09	27.9

4.2 Results

The results of the testing show the shim was able to secure the groove mount to a significant extent. The magnetic model predicted an applied force of 1.27 N from both of the tabs. By performing a force balance in the lateral case, the increase in magnetic attraction can be determined.

With Shim	Without Shim
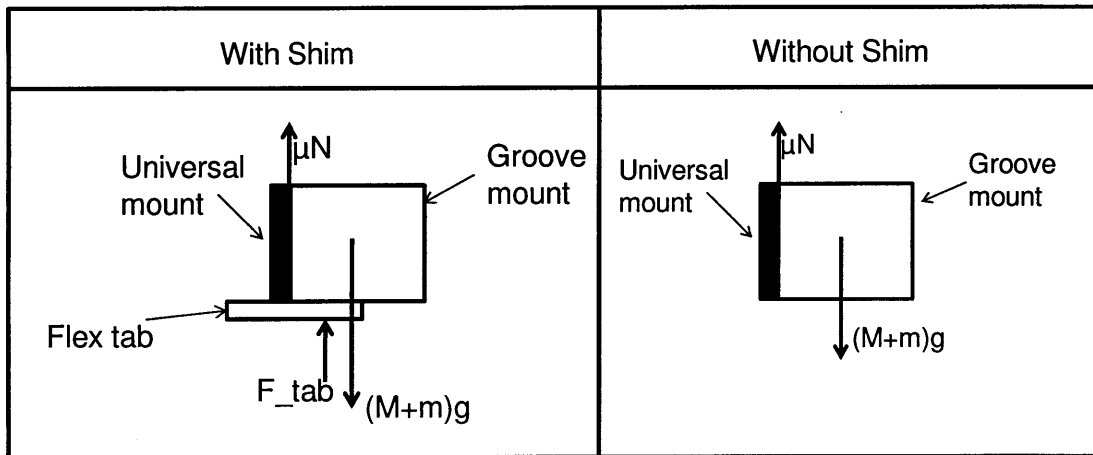
Figure 19: Free body diagrams for the shim in the lateral loading condition.

Balancing the forces for the configuration with the shim yields

$$-mg + F_{tab} + \mu N = 2.45\ N \ , \qquad\qquad [8a]$$

and solving for the friction force:

$$\mu N = 1.18\ N \ . \qquad\qquad [8b]$$

Similarly for the shim-less configuration:

$$-mg + \mu N = 0.09\ N\ ,$$ [9a]

and

$$\mu N = 0.09\ N\ .$$ [9b]

The coefficient of friction, μ, is the same in both instances. Dividing the two friction forces will thus produce the ratio of normal forces. From Equation [1], it is possible to see that the value should approximate the square of the increase in magnetic flux. Using this method, the magnetic flux increases by a factor of 3.8 with the addition of the shim. Looking back to the magnetic modeling section, the shim-less configuration registered a magnetic flux of 0.08 T compared to a flux of 0.31 T for the configuration with the shim. Dividing these two fluxes produces a factor of 3.9 for an error of 2.6%. The close proximity of these two results serves to validate the model. Converting these ratios back to an increase in magnetic force, one finds a factor of 14 and a factor of 15 for the experimentally derived and magnetic modeled derived approaches, respectively.

Chapter 5: Conclusion

The purpose of this work was to develop a viable solution to the issue of groove mount dislocation. It is important to maintain the precision of the tool tip location to maintain the overall precision of the machine; if the tip is easily disturbed, the nanopositioner will be unable to produce features on scales of less than 100 nm. The addition of the shim is a significant improvement over the previous design because the groove mount is now secure when it is put in place. The shim allows the tool to be easily changed without sacrificing the precision of the kinematic coupling. As a result, the nanopositioner is both more precise during operation and more practical to use.

The vertical and lateral constraint on the groove mount improved dramatically as a result of the shim. Early estimates predicted the magnetic force could be increased by a factor of 5.6 simply by adding tabs that decreased the resistance between the magnet and groove mount in the magnetic circuit. This estimation was based on the flux proportionality argument (section 3.2) and was significant enough to warrant further investigation. By designing the tabs to press against the groove mount, the magnetic force was predicted to have increased by a factor of 14 using similar reasoning. Using an experiment, the vertical force required to displace the groove mount increased by a factor of 9.4, from 0.14 N to 1.29 N. Similarly the lateral force increased by a factor of 27.9, from 0.09 N to 2.45 N.

The mechanical loading is designed to supplement the magnetic attraction. As such, the combined mechanical and magnetic displacement loads should be greater than the magnetic displacement loads by a factor greater than that of the estimated increase in magnetic attraction. While the load factor for the lateral testing behaves as expected, the vertical load factor is less than expected by 33% (9.4 vs. 14). This discrepancy may have been caused by the loading of the weight onto the groove mount. In the vertical orientation, it is much easier to displace the shim as the shim tabs provide less mechanical force in the corresponding direction. Further investigation is required to determine the exact breakdown of mechanical and magnetic forces holding the groove mount in place.

From a qualitative perspective, the groove mount feels secure with the shim in place. It snaps into place with ease and stays there unless it is intentionally removed. It is immune to both lateral dislocation, and being pulled off by the attraction of the ball mount magnet. In addition to increasing the forces required to dislocate the groove mount, the shim also met the other design parameters. The shim was designed with a corrosion resistance material that was able to produce the applied force within the required deflection range. In this manner, the shim successfully achieves its function.

Future work involves looking at ways to simplify the production of the shim. In the current state, bending the tabs to the desired position is somewhat tedious. While nesting the flex tabs provided the desired mechanical characteristics, it also increased the number of bends, and thus bending operations, from one to three. The increased number of bends increased the complexity of the fabrication process. The first bend can easily be achieved to within half a degree, but subsequent bends using pliers are less precise. The gap between the two flex tabs is 0.41 mm (0.016 in). If the shim was bent and then placed in a fixture, it might be possible to fold the tab over a piece of sheet metal equal in thickness to the gap between flex tabs. Until this fixture is designed, each shim must be bent into shape with pliers. In addition to reducing the time to produce the finished shim, the fixture would be reusable and thus greatly improve fabrication if greater quantities were needed for more nanopositioners.

Chapter 6: References

[1] Anderson, G. 2003. A Six Degree of Freedom Flexural Positioning Stage. Master's Thesis, Massachusetts Institute of Technology, Cambridge. 2 p.

[2] Belendez, Tarsicio, Cristian Neipp, and Augusto Belendez. Large and small deflections of a cantilever beam. 8 May 2002. 377 p.

[3] Clarke, R. The force produced by a magnetic field. 7 March 2004. Web. 30 April 2010

[4] Culpepper, Martin. 2.72 Elements of Mechanical Design Lecture 05: Structures. 15-39 pp.

[5] Culpepper, Martin. Magnetic Behavior of Stainless Steels, Austenitic, Ferritic, Martensitic, and Precipitation Hardenable Stainless Steels. Magnetic Component Engineering, Inc. Web. 30 April 2010.

[6] Culpepper, Martin, and Gordon Anderson. Design of a low-cost nano-manipulator which utilizes a monolithic spatial compliant mechanism. 2005.

[7] Hibbeler, R. C. Mechanics of Materials. 6th Ed. Upper Saddle River, NJ: Pearson Prentice Hall. 2005.

[8] Oberg, Erik, Franklin D. Jones, Holbrook L. Horton, and Henry H. Ryffel. Machinery's Handbook. 25th Ed. New York, NY: Industrial Press Inc. 1996. Print.

[9] Shigley, Joseph E., et al. Mechanical Engineering Design. 8th Ed.

[10] Short History on Nanotechnology. The Foresight Institute. Web. 30 April 2010 <http://www.foresight.org>.

Appendix A: Shim Drawing

The following diagram depicts the shim and associated dimensions. The base of the shim mimics the base of the universal scanning head on which it is placed. The holes are sized to prevent interference with the screws that secure the universal mount to the universal scanning head. The shim tab dimensions are a result of the optimization process developed within this thesis.
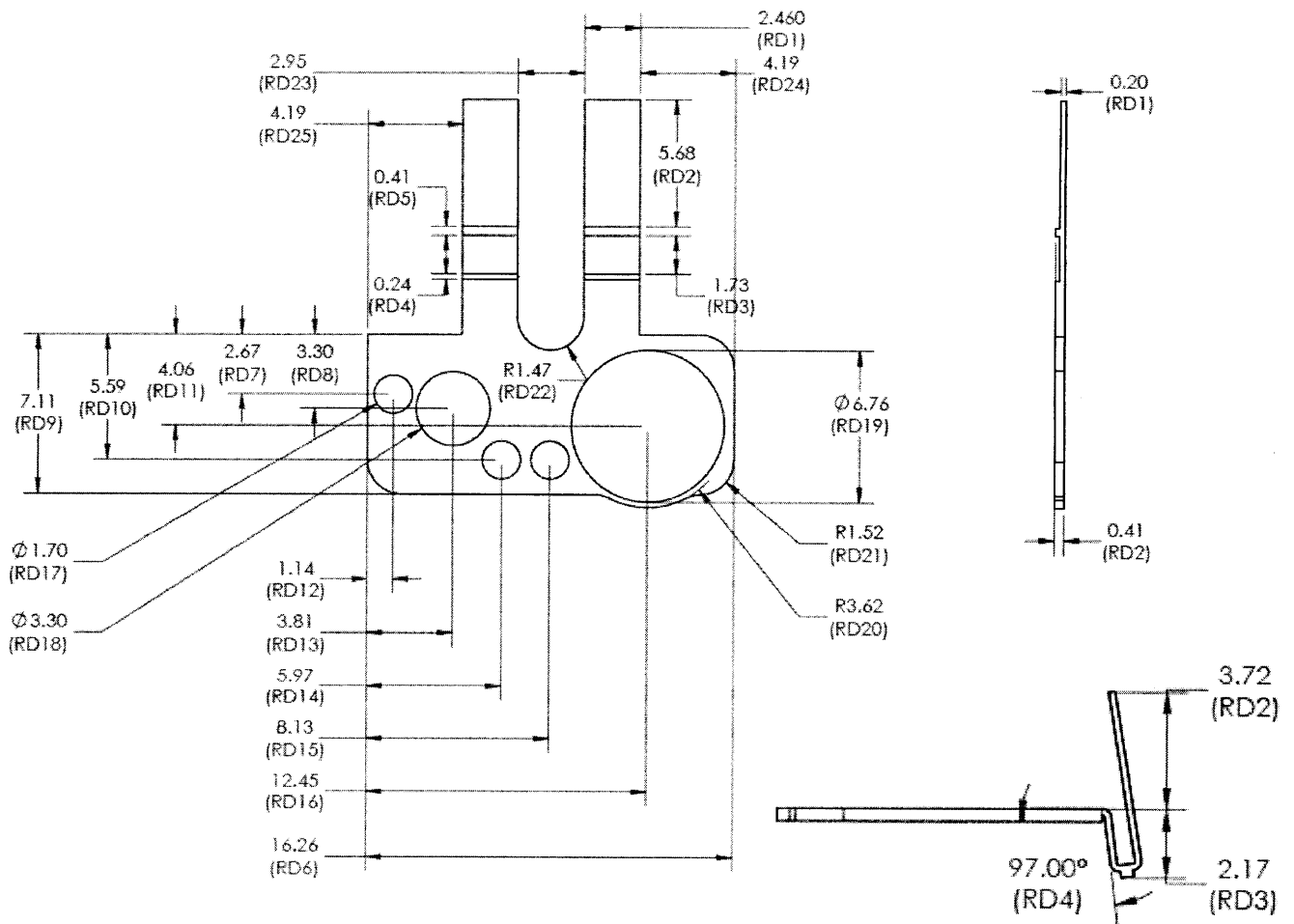

Figure 20: Shim drawing in flat and bent configurations.

Appendix B: Homogeneous Transformation Matrices (HTM's)

The shim tabs were modeled with the assistance of HTM's discussed in section 2.4.1. The following parameters are a result of the optimization with the assistance of MathCAD. The first section specifies the geometry and is followed by the HTM's themselves. These are combined to produce the deflection at the bottom of the page. Furthermore, it is possible to methodically update the applied force in the MathCAD file and calculate the corresponding deflection.

Geometry

$F = 0.831\ N$

$L_1 = 5.61\ mm$ $t_1 = 0.203\ mm$

$L_2 = 0.406\ mm$ $t_2 = 0.0406\ mm$

$L_3 = 1.84\ mm$ $t_3 = 0.203\ mm$

$L_4 = 2.464\ mm$ $t_4 = 0.0406\ mm$

$w = 2.46\ mm$
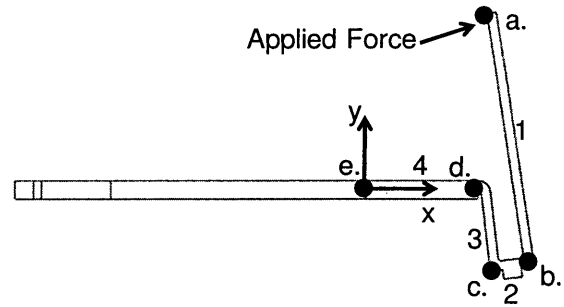
HTM's

$$H_a = \begin{bmatrix} 0.999 & 0.037 & 1.398 \times 10^{-4} \\ -0.037 & 0.999 & 5.61 \times 10^{-3} \\ 0 & 0 & 1 \end{bmatrix}$$

$$H_b = \begin{bmatrix} 1 & 3.382 \times 10^{-4} & 4.06 \times 10^{-4} \\ -3.382 \times 10^{-4} & 1 & -1.373 \times 10^{-7} \\ 0 & 0 & 1 \end{bmatrix}$$

$$H_c = \begin{bmatrix} 0.995 & -0.101 & -1.763 \times 10^{-5} \\ 0.101 & 0.995 & -1.84 \times 10^{-3} \\ 0 & 0 & 1 \end{bmatrix}$$

$$H_\theta = \begin{bmatrix} 0.993 & -0.122 & 0 \\ -0.122 & 0.993 & 0 \\ 0 & 0 & 1 \end{bmatrix}$$

$$H_d = \begin{bmatrix} 1 & 2.649 \times 10^{-3} & 2.464 \times 10^{-3} \\ -2.649 \times 10^{-3} & 1 & 3.58 \times 10^{-6} \\ 0 & 0 & 1 \end{bmatrix}$$

$$H_{total} = H_d H_\theta H_c H_b H_a = \begin{bmatrix} 0.983 & -0.182 & 1.971 \times 10^{-3} \\ 0.182 & 0.983 & 3.768 \times 10^{-3} \\ 0 & 0 & 1 \end{bmatrix}$$

Deflection

$$\Delta X = 0.2445\ mm$$
$$\Delta Y = 0.05304\ mm$$
$$Total\ Deflection = \sqrt{\Delta x^2 + \Delta y^2} = 2.502\ mm$$

Appendix C: Material Properties 17-7 PH Stainless Steel

The following table details the material properties of 17-7 PH Stainless Steel. This steel was chosen for its high strength, corrosion resistance, and magnetic properties.

Table 4: Material properties of 17-7 PH Stainless Steel, Condition A.

17-7 PH Stainless Steel Condition A (annealed)		
Minimum Properties	Ultimate Tensile Strength, psi	130,000
	Yield Strength, psi	40,000
	Elongation	35%
	Rockwell Hardness	B85
Chemistry	Iron (Fe)	70.59 - 76.75%
	Carbon (C)	0.09% max
	Chrome (Cr)	16 - 18%
	Aluminum (Al)	0.75 - 1.5% max
	Manganese (Mn)	1% max
	Nickel (Ni)	6.5 - 7.75%
	Phosphorous (P)	0.04% max
	Sulphur (S)	0.03% min
	Silicon (Si)	1% max

Appendix D: List of Variables

The following is a list of variables used within this document.

N normal force [N]

μ_0 permeability of free space [H/m]

μ_r permeability of material

g gravitational acceleration [m/s^2]

m mass [kg]

μ coefficient of friction

F_{tab} tab force [N]

σ_{max} maximum stress [Pa]

E Young's Modulus [Pa]

δ lateral deflection [m]

t thickness [m]

F force [N]

I area moment of inertia [kg·m^2]

R reluctance [A·turns/Wb]

V_m magnetomotive force [A]

φ magnetic flux [Wb]

F_m magnetic force [N]